

A High-resolution 3D Printable Porous Biomaterial

Guoyao Chen

A thesis

submitted in partial fulfillment of the
requirements for the degree of

Master of Science in Chemical Engineering (Data Science)

University of Washington

2020

Reading Committee:

Buddy D. Ratner, Chair

Cole A. DeForest

Program Authorized to Offer Degree:

Chemical Engineering

© Copyright 2020

Guoyao Chen

University of Washington

Abstract

A High-resolution 3D Printable Porous Biomaterial

Guoyao Chen

Chair of the Supervisory Committee:
Buddy D. Ratner
Chemical Engineering and Bioengineering

Three-dimension (3D) printing is a novel method to fabricate biomaterials with complex shapes and architectures. A porous biomaterial with 40 μ m pore size has been found to have good performance in reducing the foreign body reaction upon implantation, and since the inner structure is regular, a stereolithography 3D printing system was tried to print this high-resolution structure. This work has demonstrated with the laser intensity at 1×10^{-6} % and the writing speed at 1mm/s, the top surface of this structure can be printed with the commercially available resin DS2000, but the side faces cannot be properly printed due to the photo sensitiveness of the resin. The top surface of a complex and large shape, an insulin pump catheter, was also printed well. A few 2-hydroxyethyl methacrylate (HEMA) based formulas have also been tried in the printer, though further optimization is needed to accurately print high resolution structures with HEMA.

TABLE OF CONTENTS

List of Figures	iii
List of Tables	v
Chapter 1. Introduction	1
1.1 Biomaterials and Foreign Body Reaction.....	1
1.2 3D Printing of Biomaterials	4
Chapter 2. EXPERIMENTS	7
2.1 Materials	7
2.2 Methods.....	7
2.2.1 Design the Porous Structure.....	7
2.2.2 Stereolithography 3D Printing	8
2.2.3 Sensitive Test	9
2.2.4 Focus Test	10
2.2.5 Bridge Test.....	11
2.2.6 Recoating the vat with Polydimethylsiloxane.....	11
2.2.7 Composite Resin with Designed Formula	12
Chapter 3. Results and discussions	13
3.1 Focus Test	13
3.2 Sensitive Test	13
3.3 Bridge test	15

3.4	Printing Single Unit	16
3.5	Printing Structures in Stable Shapes	19
3.6	Printing High-resolution Porous Scaffold.....	23
3.7	Printing with Designed HEMA based Resins.....	31
Chapter 4. Conclusions		36
Chapter 5. Future plan.....		37
Bibliography		38

LIST OF FIGURES

Figure 1.1. cellular response to implanted polyHEMA	3
Figure 1.2. 6S process to synthesis the porous scaffold	4
Figure 1.3. the porous scaffold	4
Figure 1.4. different 3D printing technologies.....	5
Figure 2.1. sensitive test schematic diagram	10
Figure 2.2. focus test schematic diagram.....	11
Figure 3.1. focus test result.....	13
Figure 3.2. sensitive test results	14
Figure 3.3. comparison of bridge test results by DS2000 and DS3000.....	15
Figure 3.4. detail bridge test result by DS2000	16
Figure 3.5. single unit printed with 1 μ m slices.....	17
Figure 3.6. single unit printed with 2 μ m slices.....	17
Figure 3.7. failed single unit printed with 2 μ m slices.....	18
Figure 3.8. single unit with 60 μ m and 80 μ m printed with 3 μ m slices	18
Figure 3.9. 3 \times 3 \times 3 model with 80 μ m pore size.....	19
Figure 3.10. 10 \times 10 \times 1 model with 80 μ m pore size.....	20
Figure 3.11. 10 \times 10 \times 1 model without the middle part with 80 μ m pore size	21
Figure 3.12. 10 \times 10 \times 1 model without the middle part with 60 μ m pore size	21
Figure 3.13. the schematic diagram of the stabilization length test.....	22
Figure 3.14. the results of the stabilization length test	23
Figure 3.15. the schematic diagram of the stabilization length changed in 10 \times 10 \times 1 model with 60 μ m pore size	23
Figure 3.16. the result of 10 \times 10 \times 1 model with 60 μ m pore size.....	24
Figure 3.17. the result of 10 \times 10 \times 2 model with 60 μ m pore size.....	24
Figure 3.16. the result of 10 \times 10 \times 1 model with 60 μ m pore size with close pillar	25
Figure 3.16. the result of 10 \times 10 \times 1 model with 60 μ m pore size with far pillar.....	26
Figure 3.18. the result of 10 \times 10 \times 6 model with 40 μ m pore size.....	26
Figure 3.19. the result of the 10 \times 10 \times 3 model without the middle part with 60 μ m pore size	27

Figure 3.20. the result of the 1-layer insulin pump catheter	28
Figure 3.20. the result of the 1-layer insulin pump catheter	28
Figure 3.21. the result of the 1-layer insulin pump catheter with the velocity at 1.4mm/s	29
Figure 3.22. the result of the 1-layer insulin pump catheter with the velocity at 1.6mm/s	29
Figure 3.23. the result of the 1-layer insulin pump catheter with the velocity at 1.9mm/s	30
Figure 3.24. the result of the 6-layer insulin pump catheter with velocity at 1.4mm/s	30
Figure 3.25. the result of 10×10×1 model with HEMA, 6% EGDMA, 3% 1173	33
Figure 3.26. the result of 10×10×1 model with HEMA, 10% EGDMA, 3% 1173	33
Figure 3.27. the result of 10×10×6 model with HEMA, 100% EGDMA, 3% 1173	34
Figure 3.28. the result of 10×10×6 model with pure EGDMA.....	34

LIST OF TABLES

Table 3.1. All tested formulas with photoinitiator 819.....	31
Table 3.1. All tested formulas with photoinitiator 1173.....	32

ACKNOWLEDGEMENTS

I would like to thank everyone who helped me during these years at the University of Washington, and this thesis can never be completed if any of you were absent in my life.

First, I would like to thank my advisor, Dr. Buddy D. Ratner, for this wonderful project and opportunity he gave me, and for his thoughtful discussions about the direction of my research. I would also like to thank my mentor, Lars Crawford, who gave me guidance when I was handling the project in the first place, and he also gave me plenty of great suggestions during the whole process. The 3D printing project is teamwork and I would like to thank everyone in the team. Dr. Anna Galperin was reliable in troubleshooting the problems related to the printer operation; Dr. Felix Simonovsky was essential in analyzing the polymer chemistry; Dr. Le Zhen was good at experimental skills and can always point out the key effect of a problem. I would also like to thank Shijie Zhang, Meghan Wyatt for their previous work in the project.

Second, I would like to thank the rest members of the group. I would like to thank our lab manager Sharon Creason for the general training and daily assistance in the lab. Special thanks to Sherry Liu, Kyung-Hoon Kim, Louis Chen, Runbang Tang, Julia King, Prabhleen Kaur, Dr. Marvin Mecwan for their warm accompany in the group.

Finally, I would like to thank my parents Jinshui Chen, Shangdi Chen, and my sister, Danxia Chen, for their endless love and support.

This work was funded by the Center for Dialysis Innovation (CDI) and was supported by the Department of Chemical Engineering and Department of Bioengineering at University of Washington.

Chapter 1. INTRODUCTION

1.1 BIOMATERIALS AND FOREIGN BODY REACTION

A biomaterial was formally defined by the Clemson University Advisory Board for Biomaterials as a systematically and pharmacologically inert substance designed for implantation within or incorporation with living systems[1]. The goal of using biomaterials is to improve human health by restoring the function of natural living tissues and organs in the body[2]. There are a lot of applications of biomaterials including contact lenses, bone screw, insulin pump catheter, and the cell scaffolds which is widely used in tissue engineering. A wide range of materials are routinely used in all these applications, for the hard-tissue biomaterials are mostly made of metals, ceramics and materials like polymers are used to make soft-tissue biomaterials[3]. Biomaterials have also been manufactured into different shapes and architectures for different applications, including solid, porous, woven meshes, microspheres, etc.

Even though the dental implants, one of the most used applications of biomaterials, can be traced back to 600 A.D. in early civilizations[4], but the foundation ideas and principles of the biomaterial field were basically created within 100 years. Actually, before the aseptic surgical technique was invented by Dr. Joseph Lister in the 1860s, most of the implantations were unsuccessful due to the infection[5].

Before polymer was used in the biomaterial field, metal was the common implantation material especially for repairing long bones and joints. A variety kinds of bone fracture plates were designed in the early twentieth century accompanied by plenty of alloys that were introduced into medical practice. Vitallium was one of those alloys, and this alloy was found more biological compatible than the others and it was used in fracture repair of femoral neck surgeries in 1937 by

Dr. Smith-Petersen[6]. Similar mold arthroplastic surgeries were also performed by Judet brothers in France with the first biomechanical designed prosthesis made of an acrylic (methylmethacrylate) polymer[7]. The same type of acrylate polymer was latter widely used in the 1940s and 1950s due to its excellent biocompatibility[2].

The implantation of blood vessels was also tried with different materials in the 1950s, including polyethylene and acrylate polymer. In 1952, Voorhees, Jaretzta, and Blackmore used cloth prostheses made of different materials including Vinyon N copolymer (polyvinyl chloride and polyacrylonitrile), nylon, Teflon, Orlon, Dacron and Ivalon in vessel implantation, and they found out a pseudo- or neointima was formed by tissue ingrowth through the cloth pores. This was more biocompatible than a solid synthetic surface and can prevent further blood coagulation[8]. This discovery has led people to start researching porous biomaterials.

Nowadays, with the developments of materials and modern surgical techniques, biomaterials have been used in many fields including regeneration and organ replacement, however, after the implantation of biomaterials, it would induce a variety of host reactions including injury, blood–material interactions, provisional matrix formation, acute inflammation, chronic inflammation, granulation tissue development, foreign body reaction, and fibrosis/fibrous capsule development[9]. The foreign body reaction, which is composed of macrophages and foreign body giant cells, is the end-stage response of the inflammatory and wound healing responses following implantation.

To mitigate the foreign body reaction and improve the integration into the host tissue, porous biomaterials have been researched and developed. According to previous works in the Ratner lab, porous biomaterials have been shown to influence macrophage phenotype in a size-dependent manner, with 40 μ m porous biomaterials showing reduced collagen deposition, increased cellular

infiltration, and neovascularization[10]. The figure1.1 below shows the cellular response to implanted polyHEMA in different pore size scaffolds.

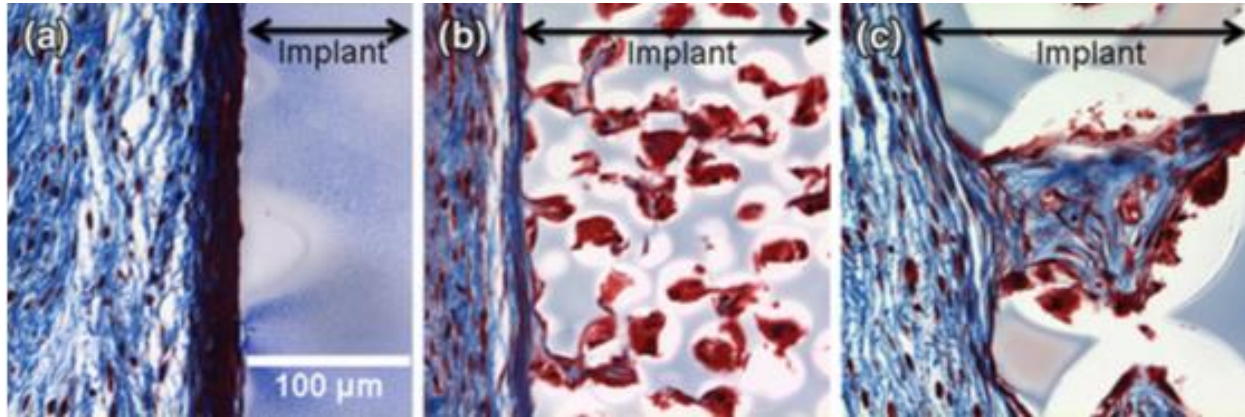


Figure 1.1. cellular response to implanted polyHEMA[10]

The 6S process is used to synthesis the 40μm porous scaffold, and the flow chart in figure 1.2 shows how the 6S process operated. The inner structure of the porous scaffold is also shown in the figure1.3 below. With the regular fabrication method, only the shapes with molds can be fabricated inside the lab. To make this structure used in a more complex architecture, a new manufacturing way is needed. Since the structure inside is regular and can be digitally designed in the computer, a new method was tried to manufacture the scaffold, three-dimensional (3D) printing.

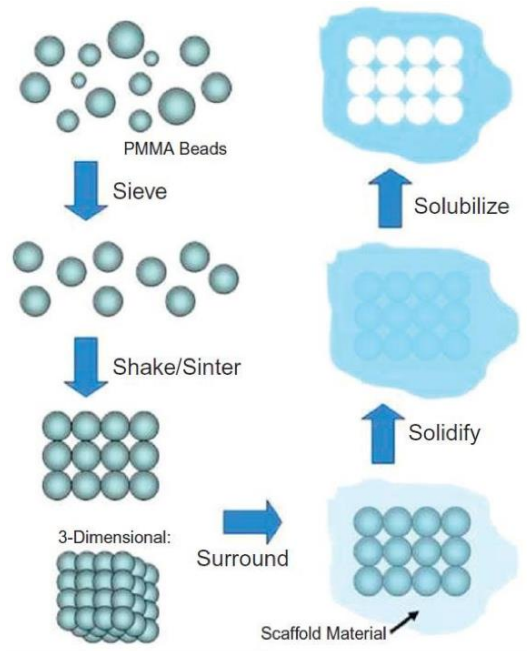


Figure 1.2. 6S process to synthesis the porous scaffold[11]

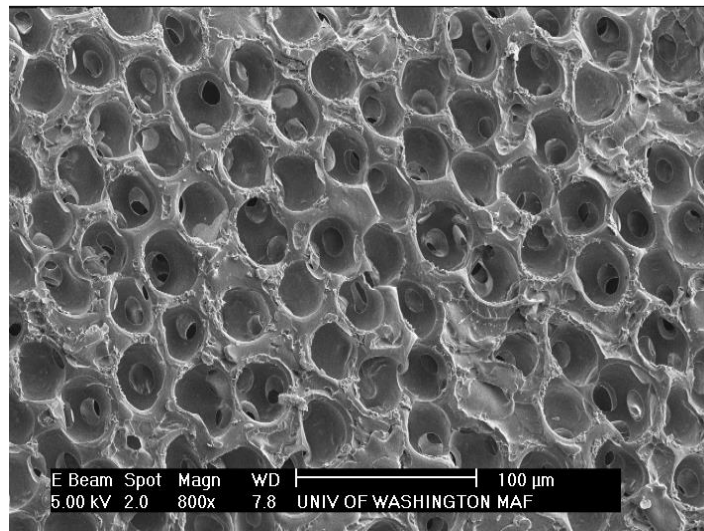


Figure 1.3. the porous scaffold[12]

1.2 3D PRINTING OF BIOMATERIALS

3D printing, also is known as additive manufacturing (AM), rapid prototyping (RP), or solid free-form technology (SFF), is a manufacturing method in which objects are made by fusing or

depositing materials—such as plastic, metal, ceramics, powders, liquids, or even living cells—in layers to produce a 3D object[13]. This technique is recognized as a versatile tool for precise manufacturing of various devices. 3D printing has been introduced in the biomedical field due to its promising to produce complex architecture and shape according to computer design. The growing demand for customized pharmaceuticals and medical devices makes the impact of 3D printing increased rapidly in recent years[14].

There are many different 3D printing methods, and basically it can be divided into 3 categories: liquid solidification like stereolithography; powder solidification like selective laser sintering (SLS); extrusion based systems. The figure below shows the main methods used in 3D printing[15].

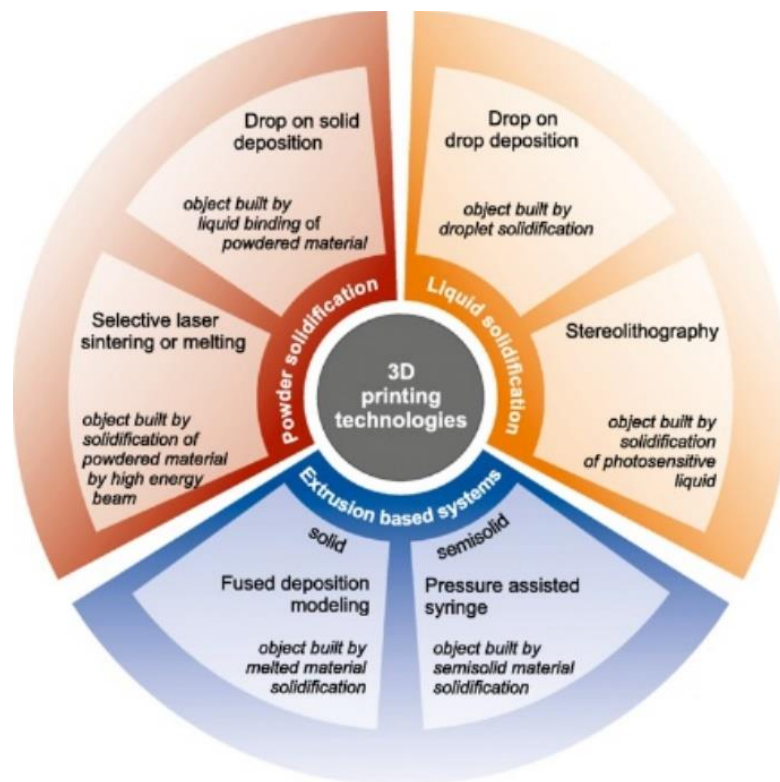


Figure 1.4. different 3D printing technologies[15]

Stereolithography (SLA) is regarded as the first rapid prototyping process and was developed in the late 1980s by Charles Hull[16]. Stereolithography uses a .stl file format to interpret the data in a computer-aided designed file, allowing these instructions to be communicated electronically to the 3D printer. Photochemical processes by which light causes chemical monomers and oligomers to cross-link together to form polymers are used in stereolithography[17]. Comparing with other 3D printing methods, while most fabrication techniques the smallest resolution are 50–200 μm in size, many commercially available stereolithography 3D printers can build objects at an accuracy of 20 μm or even lower[18]. That is why a lot of in laboratory micron-sized structures with sub-micron resolution have been fabricated using these printers[19].

As mentioned above, the porous scaffold with 40 μm pore size has been researched in the Ratner lab and it is showing reduced collagen deposition, increased cellular infiltration, and neovascularization. This work is focused on how to print the scaffold with the SLA 3D printer.

Some previous work was done by the other lab members. The scaffold unit cell with a 40 μm pore size was designed and the 10 times larger unit with 10 μm slices was printed with the KLOE high resolution 3D lithographic laser system with spatial resolution at 5 μm .

The resin DS3000 was tested in the printer before this project started. DS3000 is a photosensitive resin commonly used in 3D printing especially for dental implants due to its good biocompatibility[20, 21]. Like DS3000, DS2000 is also widely used in the 3D printing field[22], and in this work, most of the structures are printed with DS2000.

So, the objective of this project is: printing a biomaterial with 40 μm pore size and 13 μm interconnected pore size in desired shape and architecture with an SLA 3D printing system with 5 μm spatial resolution.

A few 2-hydroxyethyl methacrylate (HEMA) based formulas are also tested in this study.

Chapter 2. EXPERIMENTS

2.1 MATERIALS

All materials used in this study are listed below. Materials were used as received unless otherwise noted.

DS 2000 Resin (DWS, 10200075, 1L) is used as the original printing resin; Acetone (Fisher Chemical, A949-4, 4L) and 2-propanol (Fisher Chemical, A451-4, 4L) are used as cleaning materials for the substrates and vats; 2-hydroxyethyl methacrylate (Polysciences, 04675-500, 500g), ethylene glycol dimethacrylate (Polysciences, 24030, 250g), Omnirad 819 (iGM Resins, 162881-26-7) and Omnirad 1173 (iGM Resins, 7473-98-5) are used as materials for own designed printing resin. Sylgard 184 (Electron Microscope Sciences, 24236-10, 1 kit) is used to recoat the vat.

All equipment used in this study is listed below.

KLOE High resolution 3D lithographic laser system, including the high-resolution 3D Printer: Dilase 3D; sec SNE-3200M Scanning Electron Microscope (SEM); Thermo Scientific Lindberg Blue M Oven; VWR Scientific Mini Vortexer; Mettler Toledo AG135 Analytical Balance.

2.2 METHODS

2.2.1 *Design the Porous Structure*

The software Blender is used to design the porous scaffold with 40 μ m pore size. To design the scaffold, a cube with 53 μ m side length is first designed in Blender, then a sphere with a radius of 20 μ m is designed near the cube. Draw the sphere and combine the center of the sphere with the center of one face of the cube. Choose the cube, modifier *Boolean* is added, and choose the

operation is *Difference*, then the first half pore is made. Repeat the same operation above: combine the center of the sphere with all other centers of the other 5 faces and 8 vertexes. Use *Boolean* to cut the pores out then a unit of the porous scaffold is made. The large porous scaffold with 40 μ m pore size is made of the units.

To expand or shrink the unit or the scaffold, change the dimensions in the operation window.

2.2.2 *Stereolithography 3D Printing*

To print the porous scaffold with the stereolithography 3D printer, the scaffold needs to be transferred into printable slices, the suitable laser writing speed, intensity and focus value need to be determined before printing.

The software 3D Slicer (originally installed with the printer) is used to transfer the scaffold into printable slices. Import the structure model (in .stl format) and input the desired maximum height. Click output in the main window, follow the instruction below:

1. In step 1, enter the reference base height of the vat inside the printer. Tick the option Create an Adhesion Layer (base), input the desired offset value and layer height. Choose the writing direction as vertical.
2. In step 2, enter the height max of the structure. Input the desired slice pitch (designed layer thickness). Since the printer detector has a detect error within 2 μ m, a minimum slice pitch is required.
3. In step 3, tick the option Attempt fixing the unclosed contours issues (RED). This is to make sure all the layers will print completely.
4. In step 4, tick the contour option if needed.
5. In step 5, tick the filling option. Choose the filling direction as vertical. Change the overlap rate if needed.

6. In step 6, enter all the desired values of start stabilization length, end stabilization length, laser modulation and writing velocity.

After finishing the steps above, click finish and output the printable slices.

All printing processes need to follow the instruction below: a pre-sanitized substrate is stick on the printing stage and put the stage inside the printer. Import the base and printable slices files into the printer software KLOE Dilase, enter all desired variables' values. Pre-set the printing stage to the height which is the same as the height of the first layer, usually is the base, and then click start. After printing, put the stage with the substrate inside 70% ethanol to remove all the rest resin attached on the surface for 10mins. Remove the substrate and dry it in room temperature, then the printing is ready to do the next experiments like SEM.

2.2.3 *Sensitive Test*

To get the suitable laser writing speed and laser intensity, the sensitive test needs to be done. The sensitive test is to print a small sample structure in the printer repeatedly with different laser speed and laser intensity to figure out the best pair of these. The sample structure is usually can be replaced by a small square. Import the 2.5 mm^2 base file into the printer software, enter modulation (laser intensity percentage) value 100 and velocity 100(mm/s). Choose a coordinate (default 0,0), then import 57 $100\mu\text{m}\times 100\mu\text{m}$ squares. 56 of these are set inside a 7×9 matrix shown as figure 2.1, the velocity of each square is transferred from 100mm/s to 1mm/s; the modulation of each square is transferred from 1 to 0. The distance between every two adjacent squares is $100\mu\text{m}$. Put the last square in one corner and enter the velocity as 15mm/s, modulation as 15, this square is used to be the reference square. After finishing the printing procedure shown above, check the structures under the optical microscope and the best square shows the optimal laser velocity and modulation value of the structure.

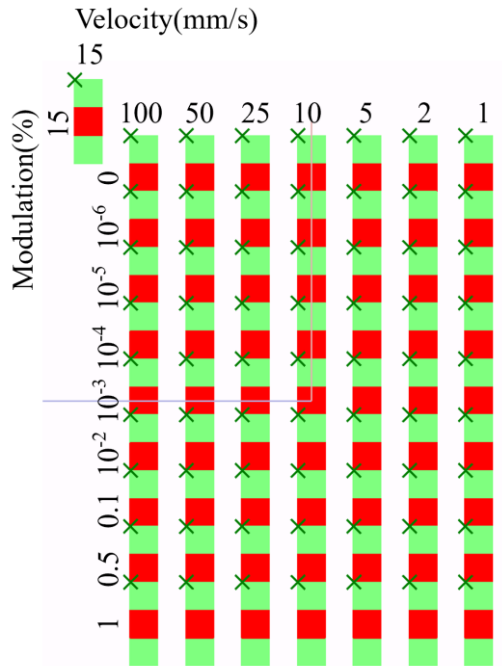


Figure 2.1. sensitive test schematic diagram

2.2.4 Focus Test

To get the suitable focus value, the focus test needs to be done. The focus test is to print a small square in the printer repeatedly with different focus values. Import the 2.5 mm² base file into the printer software, enter modulation value 100(%) and velocity 100(mm/s). Choose a coordinate (default 0,0), then import 22 100μm×100μm squares. 21 of these are set inside a matrix shown as figure 2.2, change the focus value from -1.0 to 1.0. The distance between every two adjacent squares is 100μm. Put the last square in one corner and enter the focus value to -0.2, this square is used to be the reference square. All the modulations and velocity are set as the optimal value getting from the sensitive test. After finishing the printing procedure shown above, check the structures under the optical microscope and the best square shows the optimal focus value.

After the value of the optimal variable is decided, the porous structure can be printed with all these values and do the next experiments.

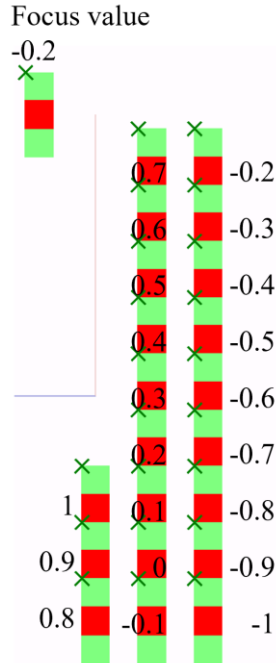


Figure 2.2. focus test schematic diagram

2.2.5 Bridge Test

To get the exact thickness of each layer, the bridge test needs to be done. The bridge test is to print a few thin bridges with desired velocity and modulation between pillars, the bridges are dangling over the base. The velocity and modulation values are gotten from the sensitive test. By taking SEM pictures of the side view of the bridge test we can get the exact thickness of each layer.

2.2.6 Recoating the vat with Polydimethylsiloxane

The original coating of the printing vat is made of Polydimethylsiloxane (PDMS), once it is damaged or broke, the vat needs to be recoated with PDMS again.

To recoat the vat with PDMS, the original coating needs to be cleaned by acetone and isopropanol until no rest polymer attached on the vat. Remove the original coating and wipe the glass with photo wiper. The PDMS polymer and harder in the Sylgard 184 kit are used to make

the coating. Weight around 16g PDMS polymer (minimum 12g) and mix it with the hardener with the ratio 10:1. After mixing, the polymer is placed in a stable area for 20-30mins to defoam. Transfer 12g of the polymer in the clean and empty vat and defoamed for 20-30mins. Meanwhile, the oven is turned on and the temperature is pre-set to 75°C, make sure the platform inside is horizontal. After defoaming in the vat, place the vat inside the pre-heat oven for 30mins, then the vat is recoated.

2.2.7 *Composite Resin with Designed Formula*

A few 2-Hydroxyethyl methacrylate (HEMA) based resins are designed and used in this study.

To composite the resin with designed formulas, 20g of HEMA is first weighted in a 50mL opaque tube with lid, then the desired amount of cross linker ethylene glycol dimethacrylate (EGDMA) is added inside the tube. Wrap the tube with foil and write the formula on the lid with formula number. The desired photo-initiator (Omnirad 819 or Omnirad 1173) with desired amount is added, and vortex the tube for 1min. Place the tube in the refrigerator if it is not used, and let it return to room temperature before using it for the next time.

Chapter 3. RESULTS AND DISCUSSIONS

3.1 FOCUS TEST

The focus value of the PDMS needs to be tested before printing anything inside the printer.

One of the focus tests result is shown in figure 3.1 below.

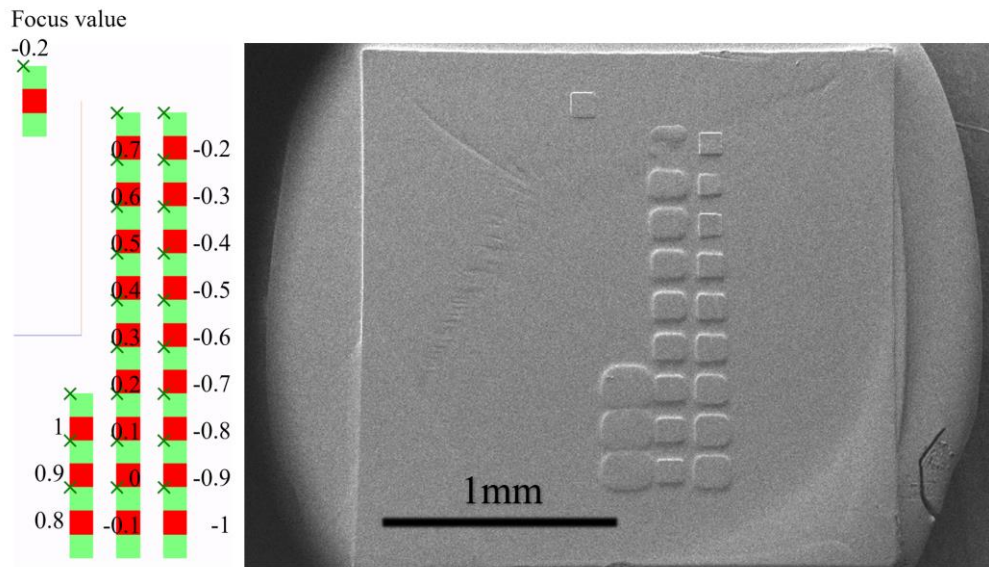


Figure 3.1. focus test result

From the figure above we can know the best focus value for this PDMS is -0.2. Pre-set the focus value inside the printer to -0.2 before all other printing.

Every time we recoat the PDMS, the new focus value needs to be tested.

3.2 SENSITIVE TEST

The optimal modulation and velocity need to be obtained by the sensitive test. By changing the layer thickness, the results of different sensitive tests are shown in figure 2.4 below.

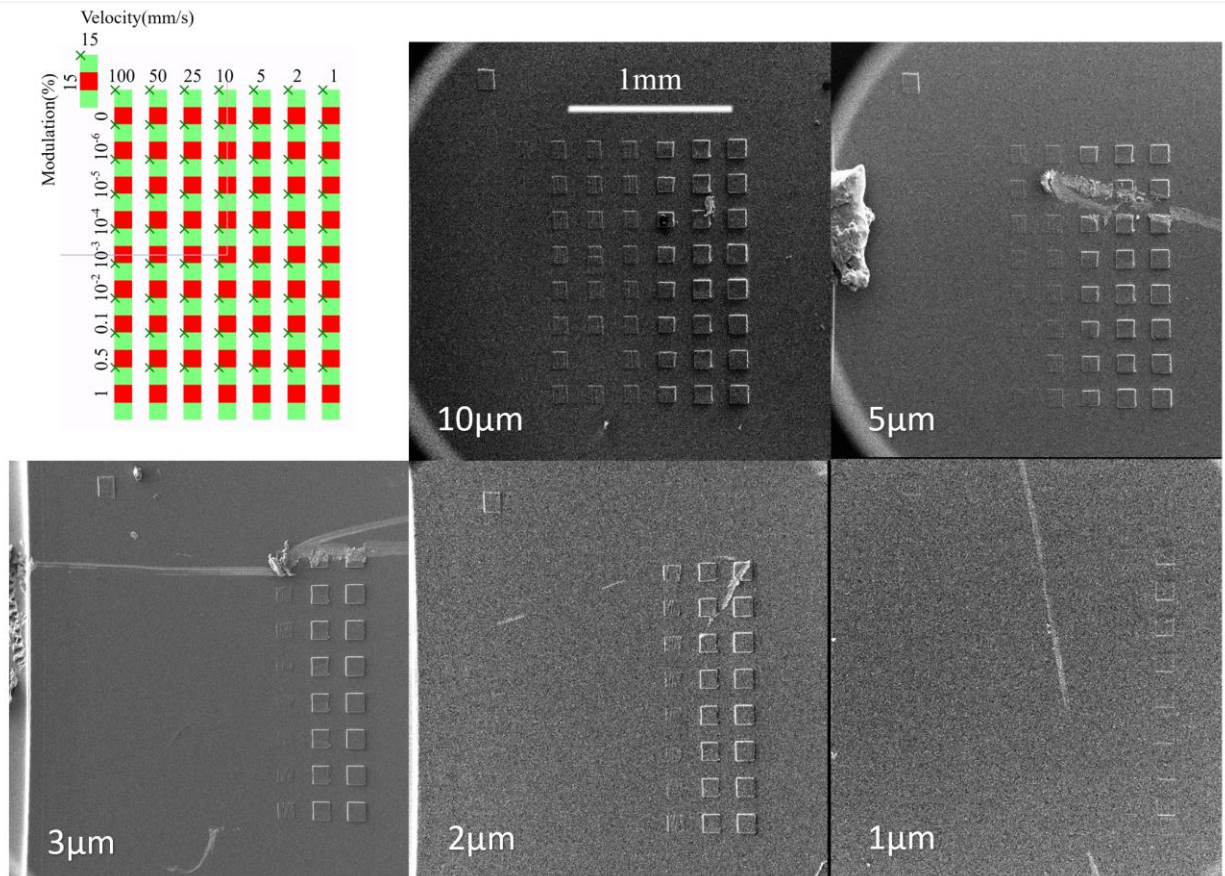


Figure 3.2. sensitive test results

From the figure above we know by changing the layer thickness from 10µm to 1µm, the velocity which can be used to print the squares are decreasing from 50mm/s in 10µm layer thickness to 1mm/s in 1µm layer thickness. This means if we want to increase the smoothness of the pores inside the porous biomaterials, the velocity needs to be decreased too. To maintain the resolution, the velocity around 1mm/s is used to print the porous biomaterial.

The result between the 2µm and 3µm layer thickness are almost the same, after checking with the exact printing stage height during the printing process, a detect error within 2µm is allowed in the software, which means the 2µm and 3µm sensitive tests were probably printed with the same layer thickness. Also we found that, if the preset stage height of the next layer is lower than the exact stage height due to the detect error, the stage will not move to the preset height when the

second layer start printing, and that's why part of the 1 μ m sensitive tests' results show nothing on the bases.

By changing the modulation with same velocity, from the figure 3.2 above we can know the differences are not obvious, which means when the layer thickness goes down to lower than 10 μ m, and the modulation goes down to lower than 1, the effect of the modulation is small. To reduce the over-polymerization caused by the high modulation, the value around 1×10^{-6} to 0.01 is used to print the porous biomaterial.

3.3 BRIDGE TEST

The resin DS2000 was used to finish to the majority part of this study, but part of the previous work of the 3D printer done by our group was using DS3000. Different resins will show different results in the bridge test. The comparison of the bridge test results done by DS2000 and DS3000 is shown in the figure below.

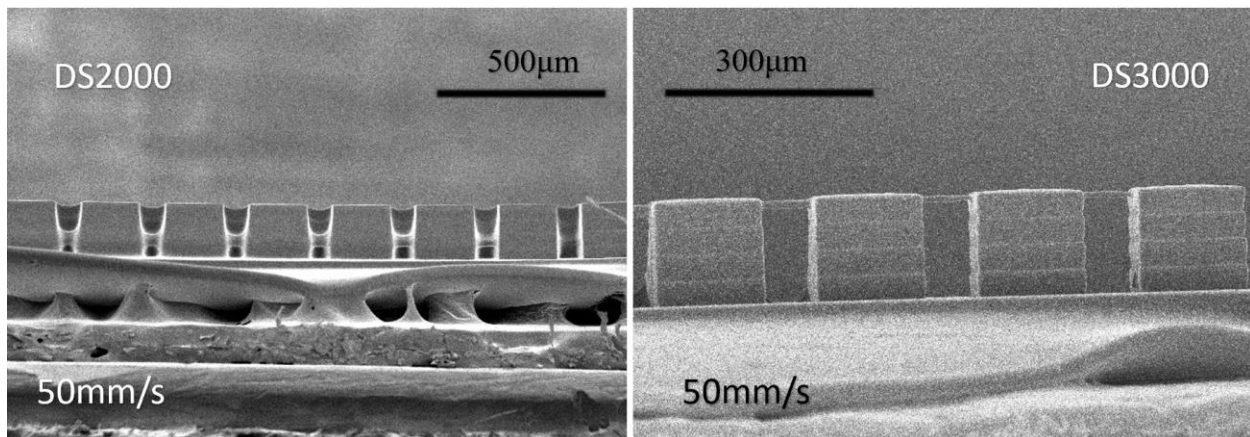


Figure 3.3. comparison of bridge test results by DS2000 and DS3000

The bridge test above were both done at the velocity 50mm/s and with different modulation. We can know DS3000 does not have a serious over-polymerization as DS2000. By reducing the

velocity to 1mm/s, which is the velocity we are using in the porous biomaterial, the result of the bridge test is shown below.

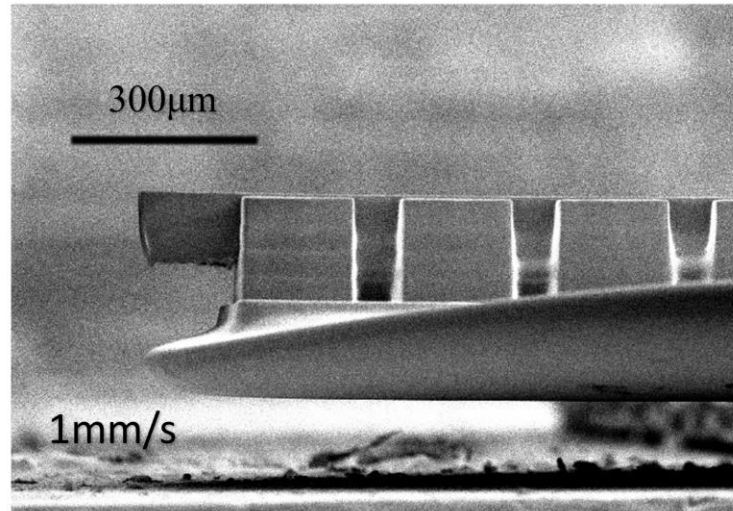


Figure 3.4. detail bridge test result by DS2000

From the bridge test result we know even with the lowest modulation, DS2000 will have an over-polymerization for about 50-100 μ m. Since this resin is originally comes from the company and is suitable for the printer, and DS3000 cannot be purchased anymore, even though the over-polymerization problem is serious, DS2000 was still using in this study.

3.4 PRINTING SINGLE UNIT

The 40 μ m pore size structure is first tried to print unit by unit. To maintain the smoothness of the pores inside, the 1 μ m slices were tried to use. The result of the unit print with 1 μ m slices is shown in the figure below.

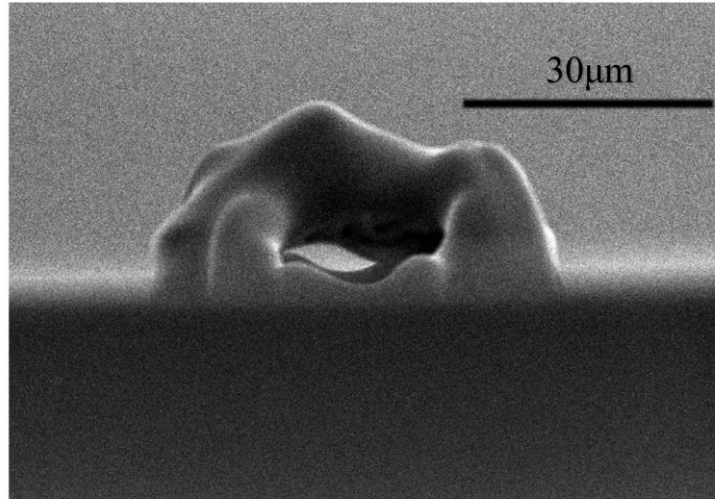


Figure 3.5. single unit printed with 1µm slices

The figure above is the only one and most successful result printed with 1µm slices. Most of the results show nothing on the base and the rest of those only show a few layers and cannot see the interconnected pores on the top of the unit in the optical microscope.

The 2µm slices were tried to print the unit next. The result of the unit print with 2µm slices is shown in the figure below.

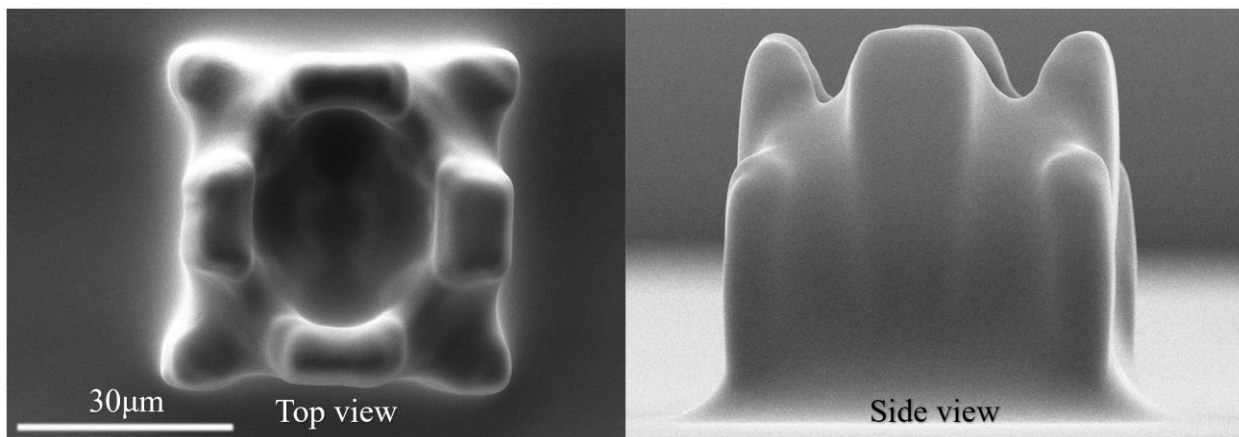


Figure 3.6. single unit printed with 2µm slices

The over-polymerization problem was shown in this result, and this is the only unit with a complete structure. Part of the failure results are shown below.

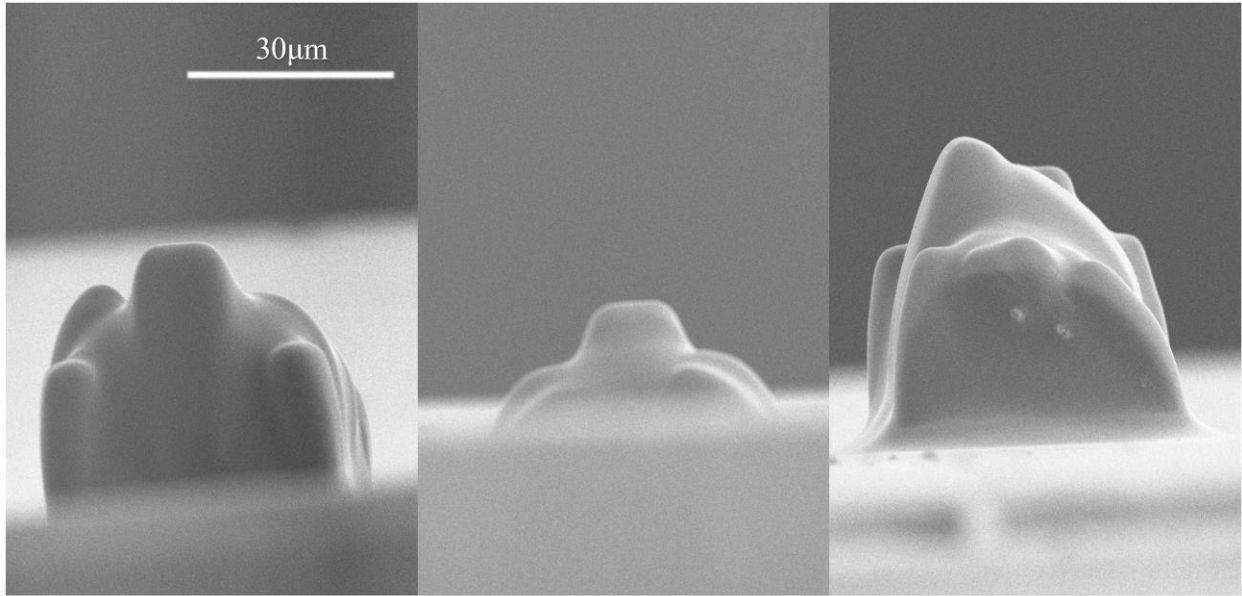


Figure 3.7. failed single unit printed with 2 μ m slices

Since the unit cannot be printed with 2 μ m slices, 3 μ m slices was chosen to print the unit and because the printer detector allows the detect error within 3 μ m, so 3 μ m layer thickness would be a stable value to use in this printer.

None of the units printed with 3 μ m slices were successful, and to continue this reserch, enlarged versions of unit were printed to test the feasibility of using this printer to print the porous structure. The results of the unit with 60 μ m pore size and 80 μ m pore size are shown below.

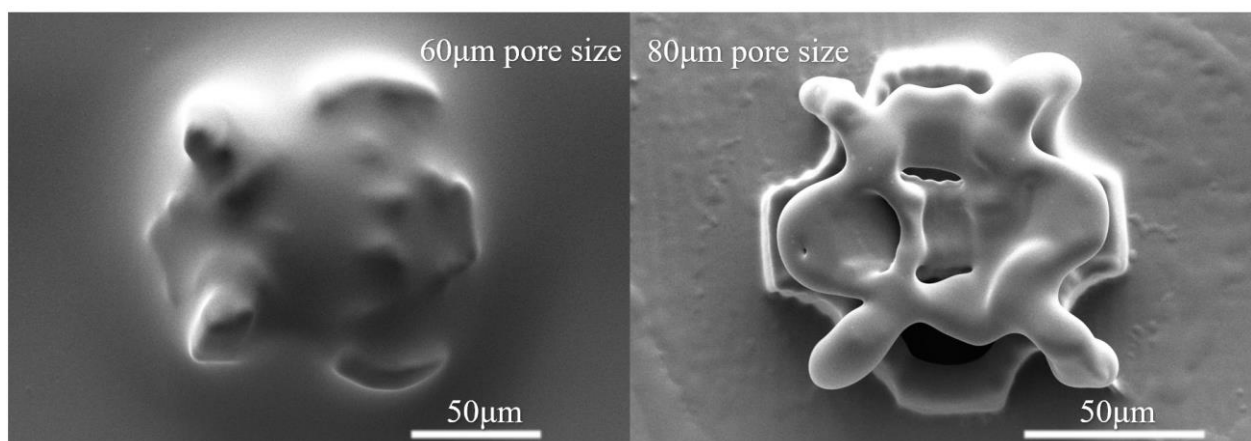


Figure 3.8. single unit with 60 μ m and 80 μ m printed with 3 μ m slices

The figure above shows that, the unit with 60 μm pore size still cannot be printed well, but when the unit is expanded to 80 μm pore size, the clear structure of the first few layers can be printed well and the upper layers are shown too. This is because the over-polymerization is only for about 100 μm and the unit with 80 μm pore size is with dimension about 106 μm . For the upper layers cannot print well was probably due to the unstableness of the upper structure of the unit, and since part of the unit is dangling, the vibration of the printer during the printing process would cause damage to the structure. This will lead to the incompleteness of the unit. Therefore, a stable structure is the key effect for this study to continue.

3.5 PRINTING STRUCTURES IN STABLE SHAPES

A 3 \times 3 \times 3 structure with 80 μm pore size was designed and printed. The result is shown in the figure below.

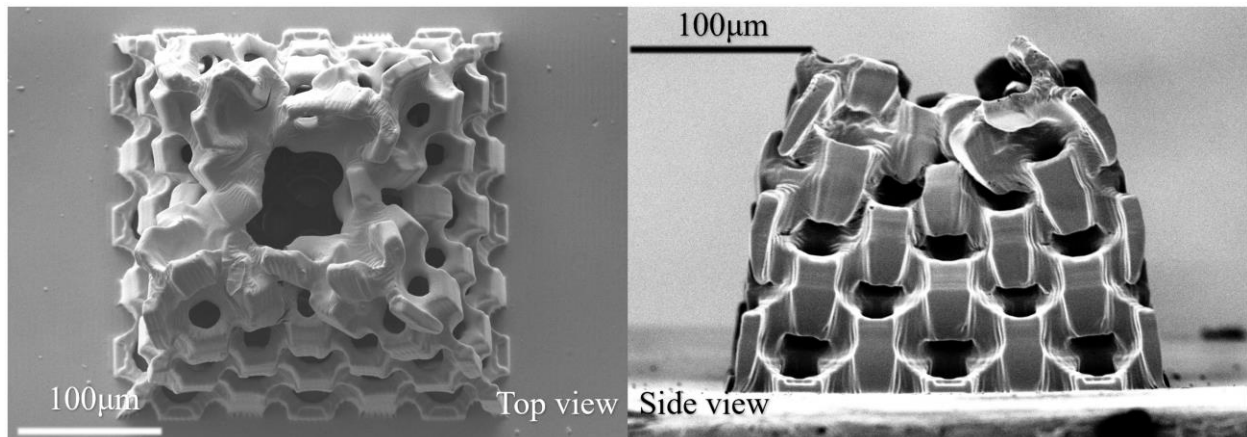


Figure 3.9. 3 \times 3 \times 3 model with 80 μm pore size

From the result above we know the over-polymerization problem is still obvious but part of the pores can be seen. The middle part of the structure is missing, it was probably because the structure is still not stable, but also was because the resin cannot flow inside. The hypothesis is, because the DS2000 is viscous and when the printer tries to print a new layer, the gap between the

printed structure and the PDMS is only $3\mu\text{m}$ and the resin needs time and a driving force to flow inside. To solve this problem, a higher velocity or a more severe vibration can help the resin to flow inside. Also, if the structure is a ring without the middle part, the problem will not show up.

To make sure the missing of middle part of $3\times 3\times 3$ model is cause by the viscosity of the resin but not the unstableness of the structure it self, a $10\times 10\times 1$ model with $80\mu\text{m}$ pore size was designed and printed to prove the hypothesis above. The result of the structure is shown in the figure below.

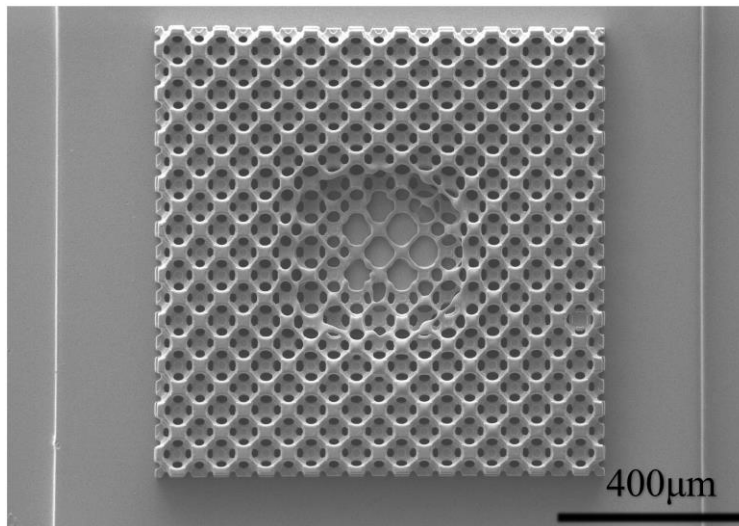


Figure 3.10. $10\times 10\times 1$ model with $80\mu\text{m}$ pore size

From the result above we know the hypothesis is correct, $10\times 10\times 1$ model is much more stable than $3\times 3\times 3$ model, but the middle part problem was also showing, which means it is cause by the diffusion of the resin. To solve this problem, a $10\times 10\times 1$ model without the middle part was designed to help the resin to flow inside the middle. The missing part is a $4\times 4\times 1$ structure. The result is shown in the figure below.

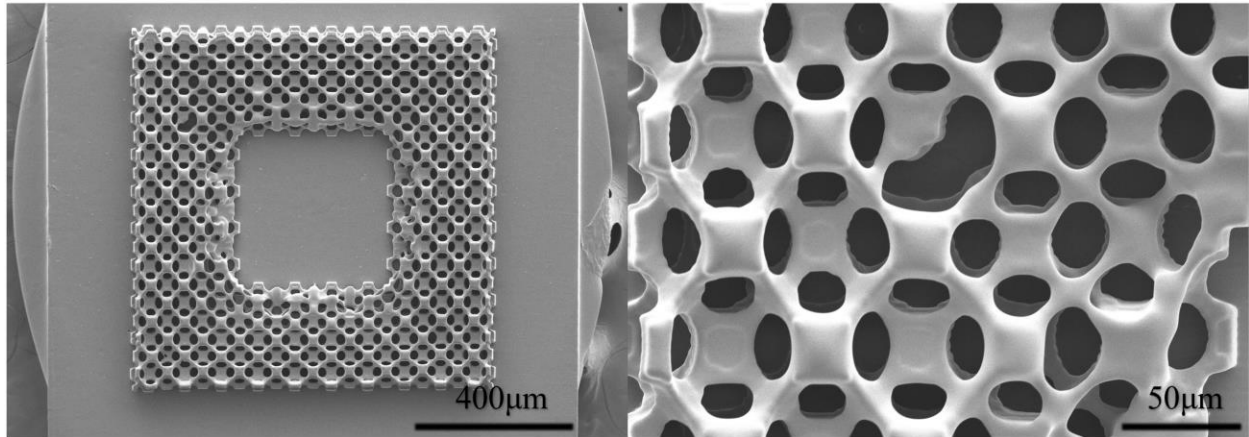


Figure 3.11. $10 \times 10 \times 1$ model without the middle part with $80\mu\text{m}$ pore size

From the result above we know that the hole in the middle cannot solve the problem but can let the structure more complete, from the detail picture of it we know part of the pores are just around $60\text{-}70\mu\text{m}$, that is because the laser beam itself has a diameter of $5\mu\text{m}$ and also because the over-polymerization in the vertical and horizontal direction, the pores are smaller than it was designed. To get the $40\mu\text{m}$ pore size biomaterial printed, a $50\text{-}60\mu\text{m}$ pore size structure is needed.

A $10 \times 10 \times 1$ without the middle part model with $60\mu\text{m}$ pore size was designed and printed. The result is shown in the figure below.

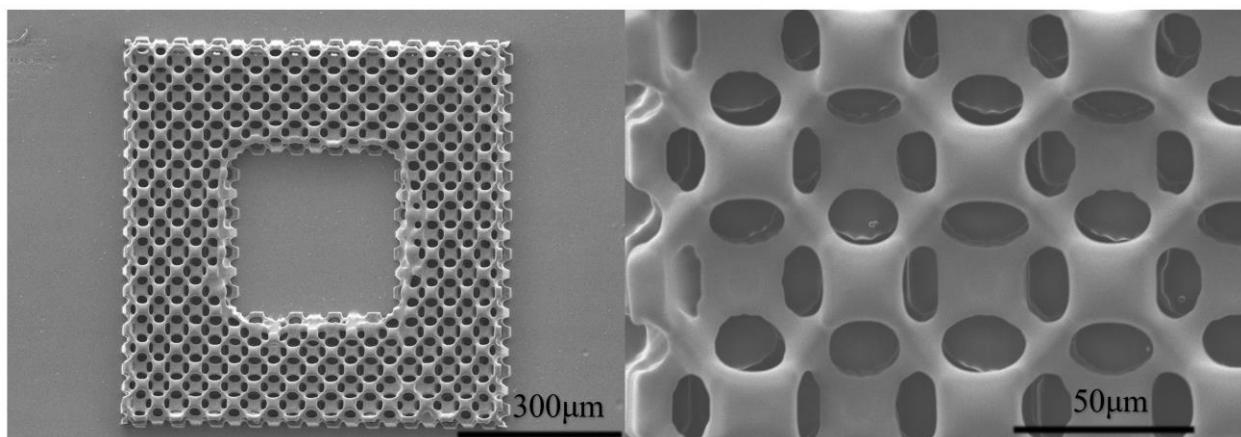


Figure 3.12. $10 \times 10 \times 1$ model without the middle part with $60\mu\text{m}$ pore size

From the result above we know most of the pores are with the diameter less than $50\mu\text{m}$ and some of those are around $40\mu\text{m}$, but the structure itself is still not complete.

By reducing the start stabilization length and end stabilization length of every printable layer, when the velocity remain the same, the printing time will be much shorter, and by reducing the printing time, the moving frequency of the laser will increase accompany with sever vibration of the printer. The hypothesis is the vibration will give the resin a driving force to flow beneath the printed structure to mitigate the diffusion problem. The default stabilization length of each layer is $50\mu\text{m}$. A test was designed to prove the hypothesis above. Multiple $500\mu\text{m} \times 500\mu\text{m} \times 50\mu\text{m}$ squares were printed in this test with different stabilization length from 1mm to 0.005mm shown as the figure below. The green parts are the stabilization length and the red parts are the squares.

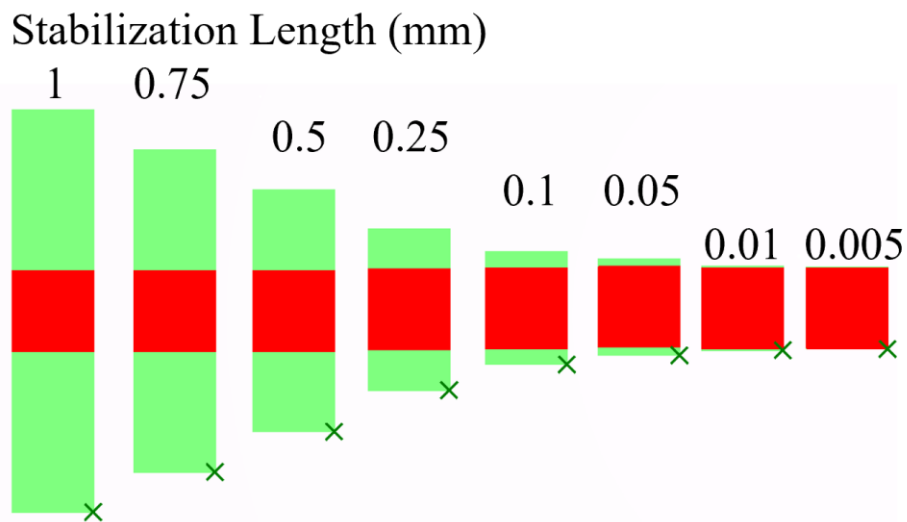


Figure 3.13. the schematic diagram of the stabilization length test

The result of the test is shown below.

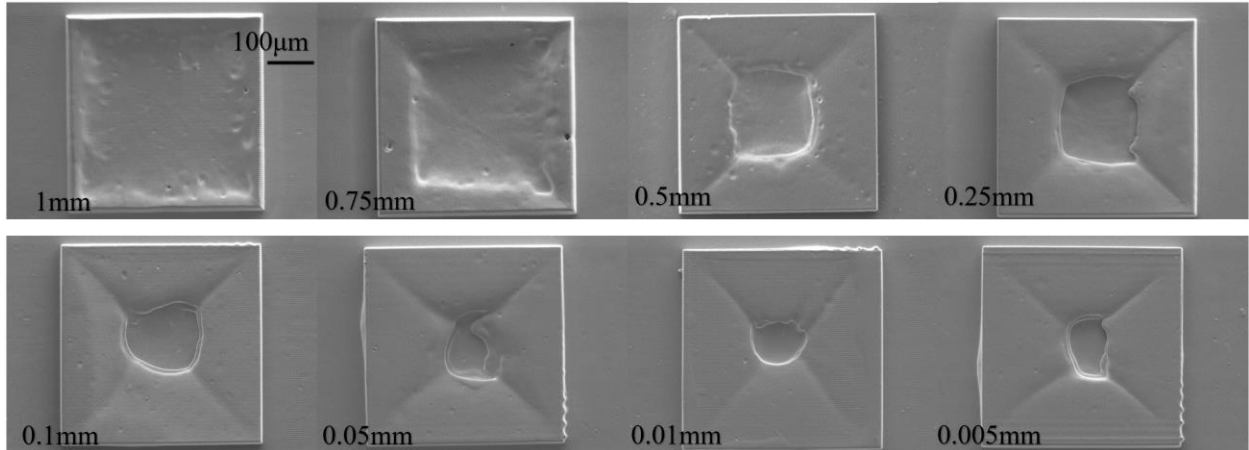


Figure 3.14. the results of the stabilization length test

From the results above we know when the velocity comes to 1mm/s, most of the structure will remain stable even when the stabilization length goes down to 5µm, and by reducing the stabilization length the diffusion problem has been significantly mitigated. Therefore, the hypothesis is correct and we can use this method to mitigate the diffusion problem of DS2000.

3.6 PRINTING HIGH-RESOLUTION POROUS SCAFFOLD

By reducing the stabilization length in the $10 \times 10 \times 1$ model with 60µm pore size from 500µm to 5µm, shown in the figure below, the result of the new model is shown below.

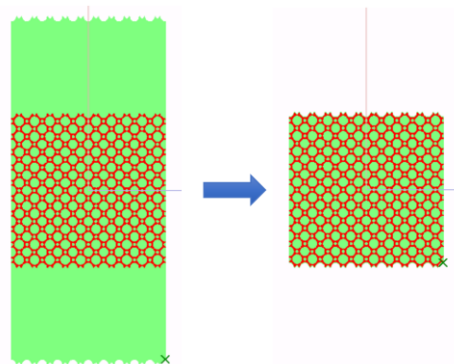


Figure 3.15. the schematic diagram of the stabilization length changed in $10 \times 10 \times 1$ model with 60µm pore size

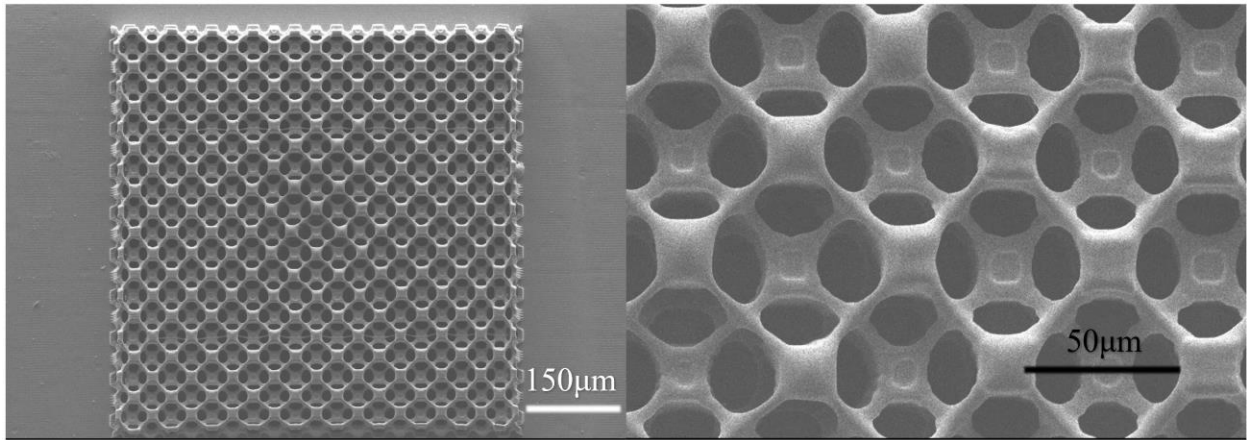


Figure 3.16. the result of $10 \times 10 \times 1$ model with $60\mu\text{m}$ pore size

We can know from the result above the structure is complete, and the diameter of the pores are around $40\text{-}50\mu\text{m}$. But this method is not always success due to the large dimension.

A $10 \times 10 \times 2$ model with $60\mu\text{m}$ pore size was designed and printed to check if the diffusion problem would happen in the higher layers. The result is shown in the figure below.

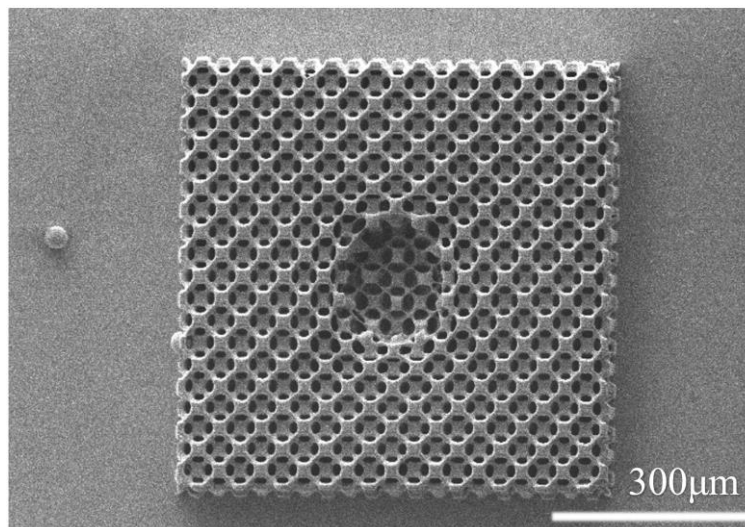


Figure 3.17. the result of $10 \times 10 \times 2$ model with $60\mu\text{m}$ pore size

From the result above we know the even when the first $10 \times 10 \times 1$ layer was printed well, but the diffusion problem still happened in the second $10 \times 10 \times 1$ layer. This means by changing the stabilization length can only mitigate the diffusion problem in small structures but cannot solve it.

Since the driving force caused by the vibration is the key to solve the diffusion problem, so an auxiliary structure, pillar, was designed close to the structure. When the printer is trying to print the structure, it should print the pillar first, since the pillar is small so it will cause a high frequent vibration, and theoretically it will solve the diffusion problem. The result is shown below.

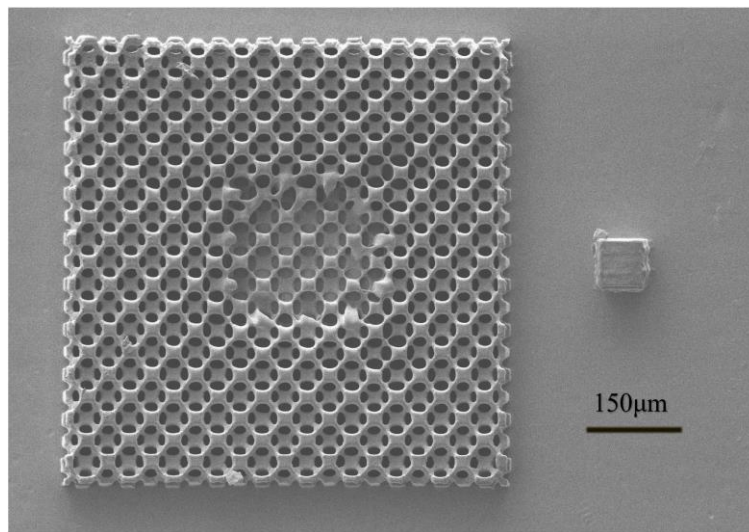


Figure 3.18. the result of $10 \times 10 \times 1$ model with $60\mu\text{m}$ pore size with close pillar

From the result we know the missing part is moving toward the pillar, so the pillar needs to be far away from the structure. A far pillar was designed, and the result is shown below.

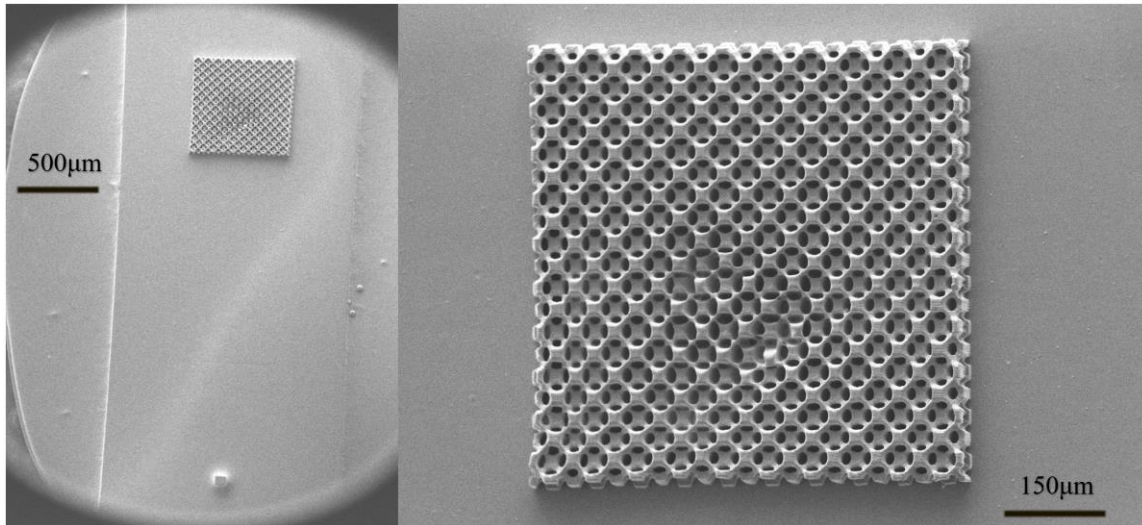


Figure 3.19. the result of $10 \times 10 \times 1$ model with $60\mu\text{m}$ pore size with far pillar

From the result above we know the structure is complete, but the diffusion problem is still happening. Since these results were printed with $5\mu\text{m}$ stabilization length, so we cannot make sure the diffusion problem is mitigated by the reducing of stabilization length or the auxiliary pillar, so more further experiments need to be done.

Since the original plan is to print a porous structure with $40\mu\text{m}$ pore size, so a $10 \times 10 \times 6$ model with $40\mu\text{m}$ pore size was designed and printed. The result is shown in the figure below.

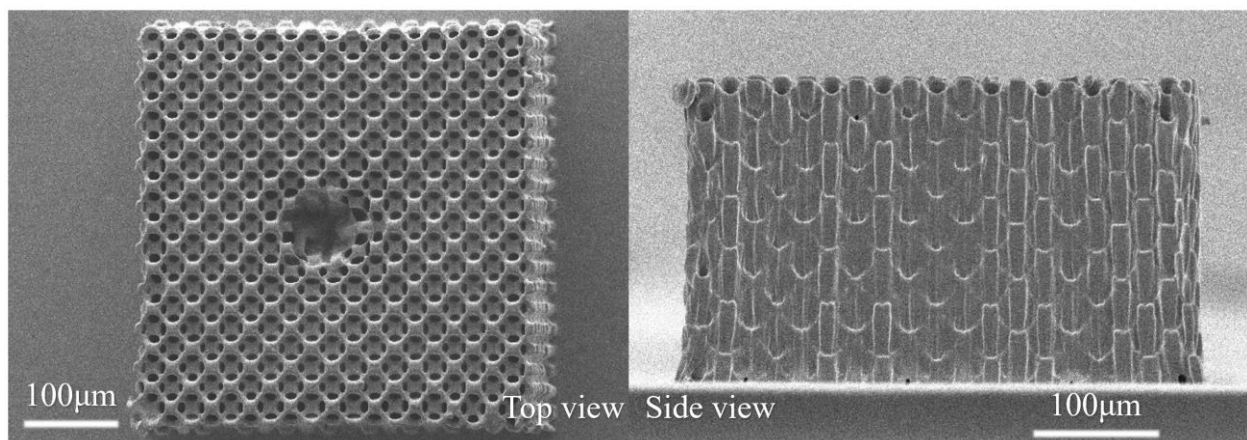


Figure 3.20. the result of $10 \times 10 \times 6$ model with $40\mu\text{m}$ pore size

From the result above we know the diffusion problem still happened in the structure with $40\mu\text{m}$ pore size, and from the sideview we can see the over-polymerization problem is serious due to the resin's photosensitiveness. But the missing part in the middle is smaller, which means if we reduce the dimension of the structure, the diffusion problem will mitigate too. But the diameter of the pores are around $30\mu\text{m}$, and that is not the desired diameter. Thus, the structure with $60\mu\text{m}$ was used in the rest of the study.

A $10 \times 10 \times 3$ model without the middle part with $60\mu\text{m}$ pore size was designed and printed to help to check the side view of the porous structure. The result is shown in the figure below.

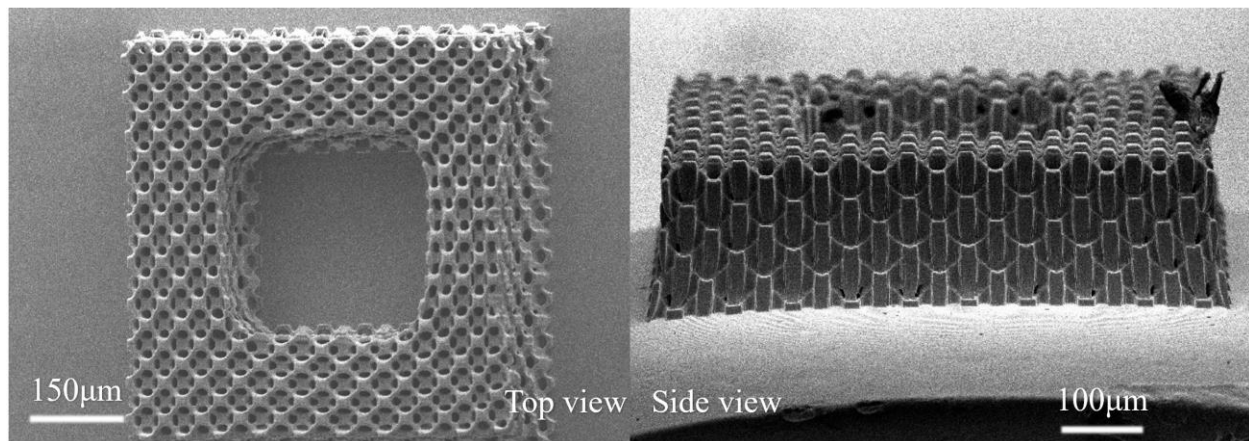


Figure 3.21. the result of the $10 \times 10 \times 3$ model without the middle part with $60\mu\text{m}$ pore size

From the result above we know the inner part of the structure is also over-polymerized but not as serious as the outer part, this is due to the resin diffusion problem.

A bigger structure, one layer of an insulin pump catheter, was designed and printed as the application shape of the porous biomaterial. The result is shown in the figure below.

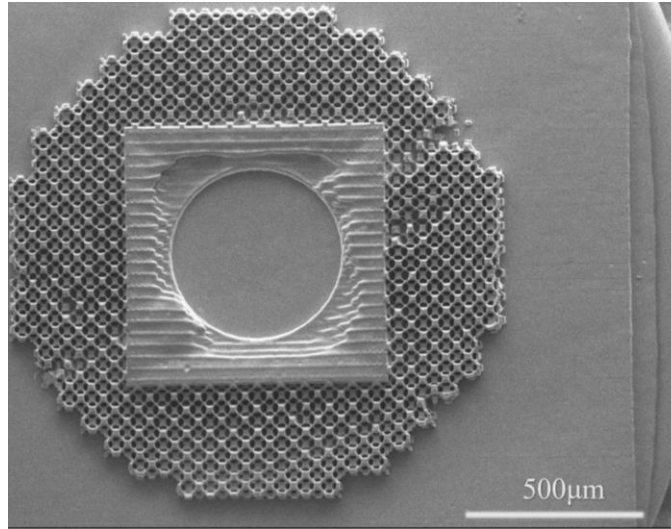


Figure 3.22. the result of the 1-layer insulin pump catheter

This structure is not complete even when it is hollow and with 5µm stabilization length, so the auxiliary pillar was tried to use in this structure. The result is shown below.

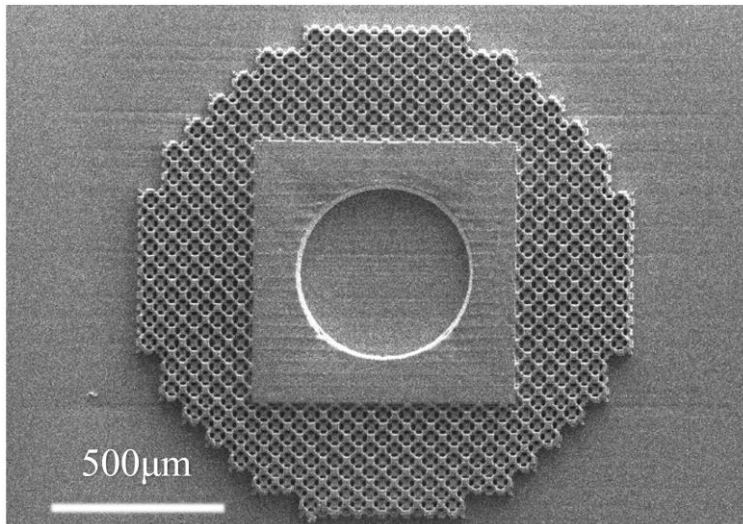


Figure 3.23. the result of the 1-layer insulin pump catheter

From the result above we know the structure is complete after using the auxiliary pillar, which means the pillar will help solving the diffusion problem.

This structure is the most complex has been tried in this study, and it was printed with modulation 1×10^{-6} and with velocity 1mm/s. The structure is complete but the printing time was

about 7 hours. To reduce the printing time, the velocity 1.4mm/s, 1.6mm/s and 1.9mm/s are all tried in this study. The results are shown below.

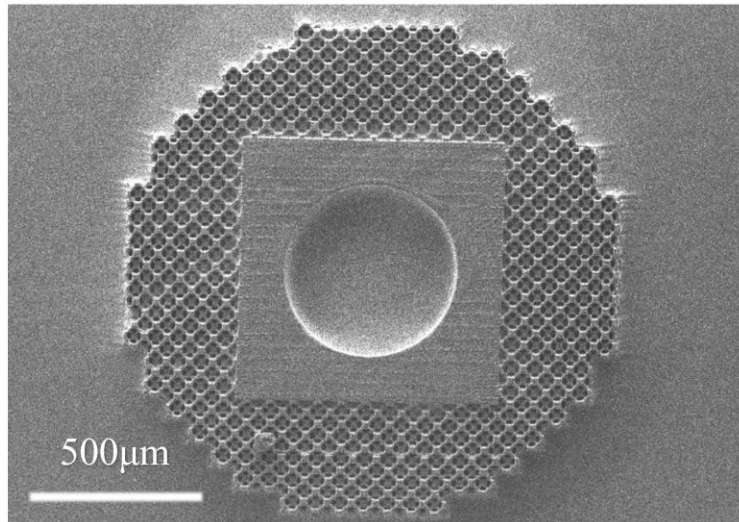


Figure 3.24. the result of the 1-layer insulin pump catheter with the velocity at 1.4mm/s

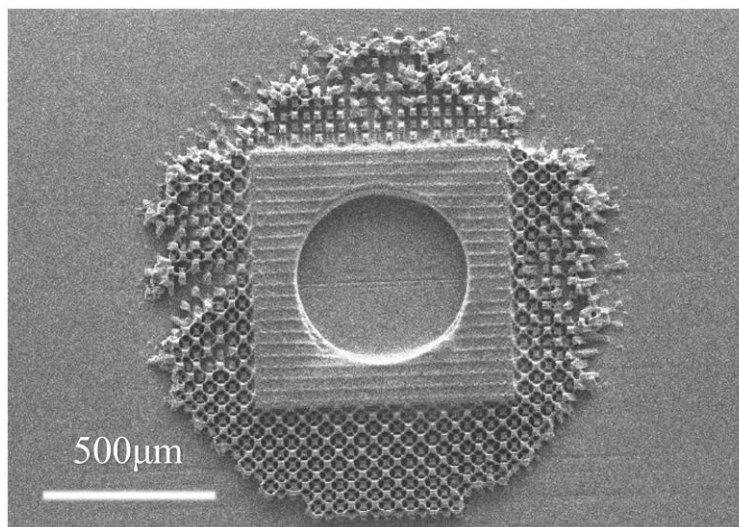


Figure 3.25. the result of the 1-layer insulin pump catheter with the velocity at 1.6mm/s

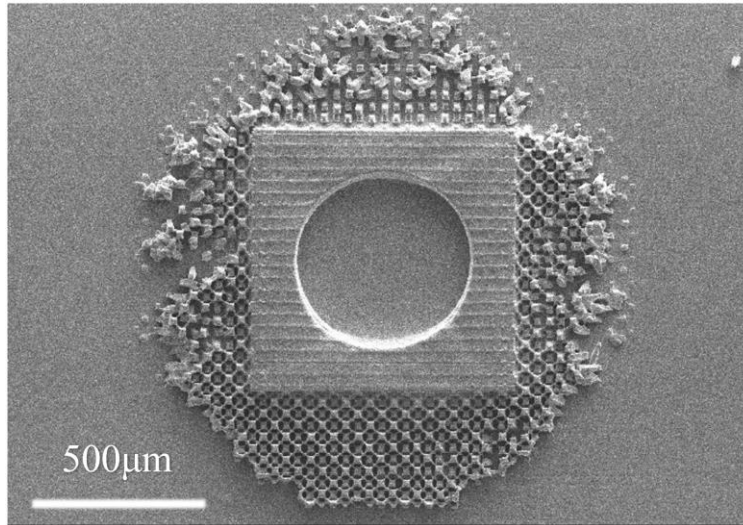


Figure 3.26. the result of the 1-layer insulin pump catheter with the velocity at 1.9mm/s

From the results above we know the structure is still complete when the velocity goes to 1.4mm/s, and the time can be reduced to about 4 hours per layer. But the structure is damaged when the velocity goes to 1.6mm/s or higher, which means the stability of the structure cannot survive under the vibration caused by the velocity which is more than 1.6mm/s. Thus, the velocity 1.4mm/s was used to print a 6 layers insulin pump catheter. The result is shown in the figure below.

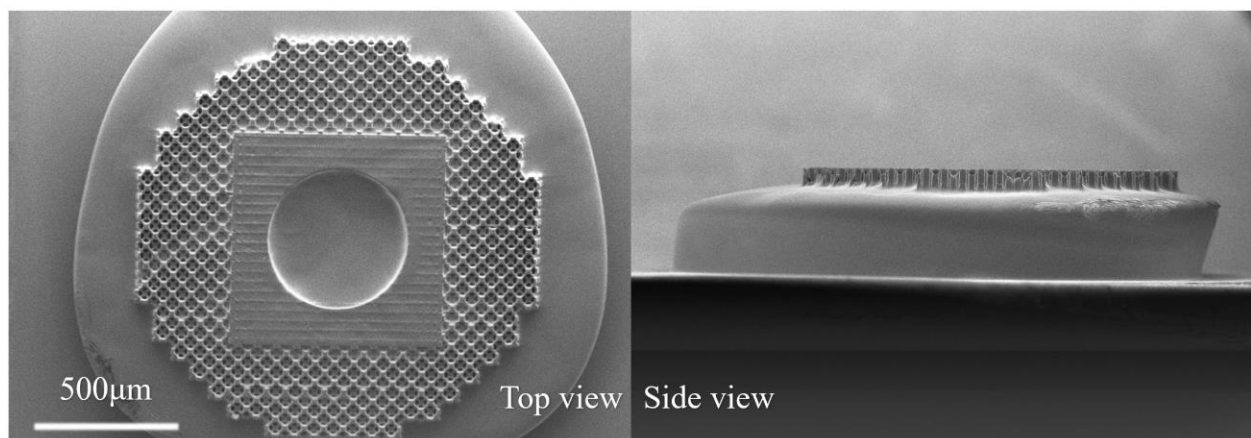


Figure 3.27. the result of the 6-layer insulin pump catheter with velocity at 1.4mm/s

From the result we know the over-polymerization problem is still serious and there is a weird base printed with the structure. This is probably because of the non-porous part inside the catheter and which means the photosensitiveness of the resin needs to be reduced to solve this problem.

3.7 PRINTING WITH DESIGNED HEMA BASED RESINS

The new formulas test is still processing, so most of the results below cannot be quantified and need further experiments to get the conclusion.

All formulas will first print with the base test (print 8 bases and see if the base is clear or not), and then do the sensitive test (50 μ m, 10 μ m, 3 μ m), if the edges with 3 μ m sensitive test are clear, then print the 10 \times 10 \times 1 model with 60 μ m pore size.

All results are showing the same problem that the base will stick to the substrate and it is hard to remove to the next step like the SEM, so only a few SEM pictures have been taken in this part.

38 new designed HEMA based formulas were tested in this study.

All the tested formulas with photoinitiator 819 are listed in the table below.

Table 3.1. All tested formulas with photoinitiator 819

Set #	HEMA(g)	EGDMA(MW ratio to HEMA)	Photoinitiator 819(mass ratio)
1	20	1%	0.20%
2	20	2%	0.20%
3	20	3%	0.10%
4	20	3%	0.20%
5	20	3%	0.30%
6	20	3%	0.40%
7	20	3%	0.50%
8	20	3%	0.60%
9	20	4%	0.20%
10	20	5%	0.20%
11	20	6%	0.10%
12	20	6%	0.20%
13	20	6%	0.30%
14	20	6%	0.40%
15	20	6%	0.50%

16	20	6%	0.60%
17	10 (with 10g water)	3%	0.20%
18	10 (with 10g water)	6%	0.20%

Photoinitiator 819 is too photosensitive and will cause a serious over-polymerization. In the sensitive tests, the concentration 0.2% of photoinitiator 819 shows the best result, but when it switched to a longer printing process, the whole substrate has been polymerized with HEMA and stuck to the printing stage, so after several experiments, photoinitiator 819 was no longer using. While using photoinitiator 819, the concentration of EGDMA has little effect.

All the tested formulas with photoinitiator 1173 are listed in the table below.

Table 3.2. All tested formulas with photoinitiator 1173

Set #	HEMA(g)	EGDMA(MW ratio to HEMA)	Photoinitiator 1173(mass ratio)
1	20	3%	0.10%
2	20	3%	0.20%
3	20	3%	0.30%
4	20	3%	0.40%
5	20	3%	0.50%
6	20	3%	0.60%
7	20	3%	1.00%
8	20	3%	2.00%
9	20	3%	3.00%
10	20	3%	4.00%
11	20	3%	5.00%
12	20	6%	0.10%
13	20	6%	0.20%
14	20	6%	0.30%
15	20	6%	2.00%
16	20	6%	3.00%
17	20	10%	0.30%
18	20	10%	3.00%
19	20	100%	3.00%
20	0	20g	3.00%

Photoinitiator 1173 is not as photosensitive as photoinitiator 819, and when the concentration goes more than 2%, some high resolution can be seen through the optical microscope, also shown in the figure below.

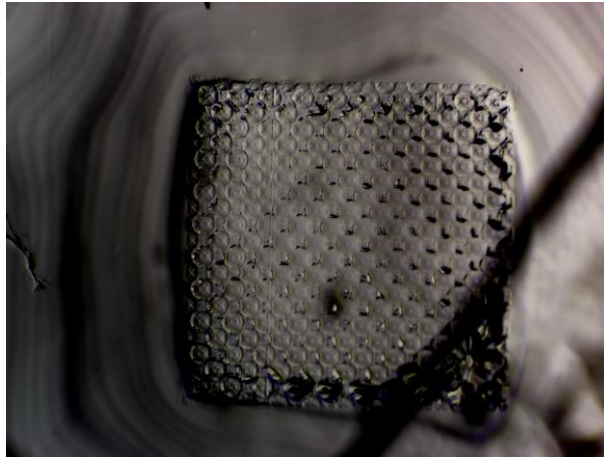


Figure 3.28. the result of $10 \times 10 \times 1$ model with HEMA, 6% EGDMA, 3% 1173

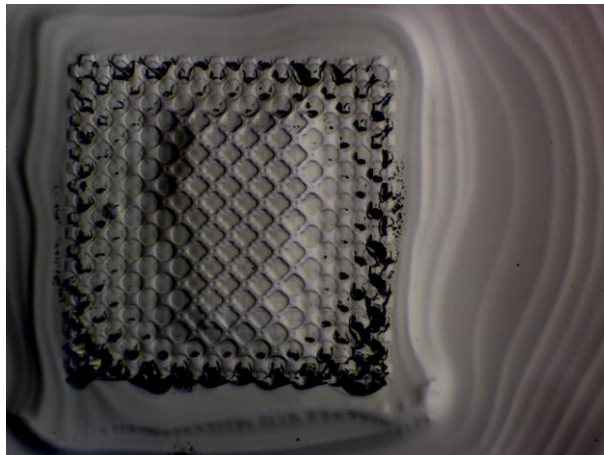


Figure 3.29. the result of $10 \times 10 \times 1$ model with HEMA, 10% EGDMA, 3% 1173

From the results above we know the structures are not complete, so more optimization process needs to be done with HEMA formulas.

While using photoinitiator 1173, EGDMA has a decent effect, 6% is much better than 3%, when using 100% EGDMA a high structure (overpolymerized) with clear edges can be printed

and can easily remove from the substrate, but part of the structure was stick to the PDMS so the structure itself is not complete either. The result of the high structure is shown in the figure below.

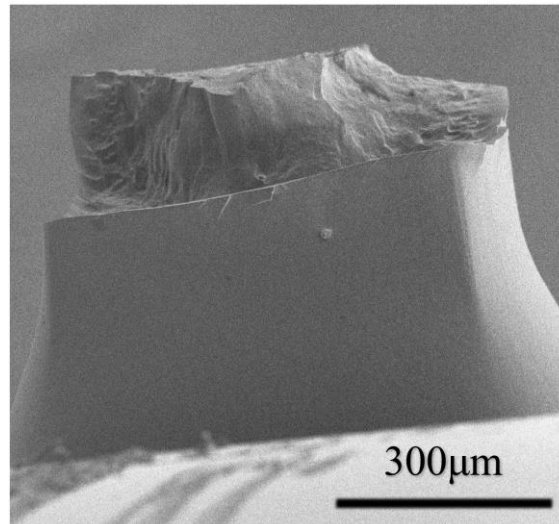


Figure 3.30. the result of $10 \times 10 \times 6$ model with HEMA, 100% EGDMA, 3% 1173

Pure EGDMA was also tried and the result is shown in the figure below. Part of the structure was also stick on the PDMS.

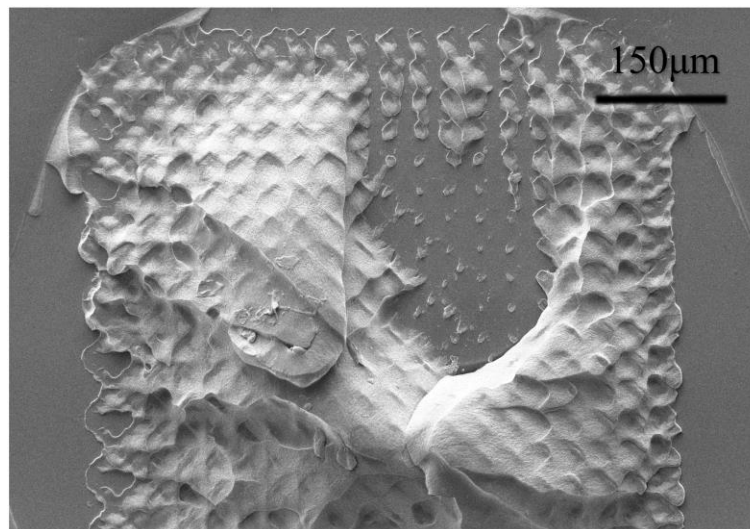


Figure 3.31. the result of $10 \times 10 \times 6$ model with pure EGDMA

When the concentration of the EGDMA is increased, the more EGDMA will penetrate inside the PDMS and the structure will stick to the PDMS, so the concentration of EGDMA needs to be optimized in the future too.

Chapter 4. CONCLUSIONS

In the study of printing a high-resolution porous biomaterial, by using the resin DS2000, the top surface of the biomaterial with 40 μ m pore size can be printed with the modulation at 1×10^{-6} and velocity at 1mm/s, but the side faces cannot be printed well due to the resin restriction. A resin with lower photosensitiveness should be tried to use in the printing to reduce the over-polymerization caused by DS2000. According to the bridge test result, DS3000 is less photosensitive than DS2000 and can be chosen as the resin used in the next step. Some conclusions are also gotten in this study.

1. The scaffold with 40 μ m pore size can be 3D printed in complex shape with fine top surface.
2. The maximum velocity to print the structure is 1.4mm/s.
3. The diffusion problem caused by the viscous resin is the main reason why most of the structures have a hole in the middle. The diffusion problem can be mitigated by giving the resin a driving force. Both reducing stabilization length and pre-print an auxiliary pillar can induce the driving force.
4. The stabilization length of each layer can be reduced to 5 μ m when the velocity goes down to 1mm/s.

Chapter 5. FUTURE PLAN

The study of the printable high-resolution porous biomaterials is still in progress, thus, a few future steps are listed below.

Short-term plans:

1. Analyze the composition of DS2000 with NMR, GC-MS, FTIR, and try to reduce the concentration of photoinitiator.
2. Optimize the HEMA formulas.
3. Increase the velocity by simplifying the structure.

Long-term plans:

1. Continue optimizing the printing process.
2. Do *in vitro* toxicology tests and *in vivo* implant studies after the biomaterial is well printed.
3. Explore cell culturing in different shape of pores.
4. Change the shape of the pores in the biomaterial to various polyhedrons and do the *in vitro* tests and *in vivo* evaluation to see if spherical pores are optimal for these structures.

BIBLIOGRAPHY

1. Park, J.B. and R.S. Lakes, Introduction to biomaterials, in Biomaterials. 1992, Springer. p. 1-6.
2. Park, J. and R.S. Lakes, Biomaterials: an introduction. 2007: Springer Science & Business Media.
3. Ratner, B.D., et al., Biomaterials science: an introduction to materials in medicine. 2004: Elsevier.
4. Bobbio, A., The first endosseous alloplastic implant in the history of man. Bulletin of the History of Dentistry, 1972. 20(1): p. 1.
5. Newsom, S., The history of infection control: Joseph Lister. British Journal of Infection Control, 2002. 3(2): p. 21-23.
6. Smith-Petersen, M., et al., COMPLICATIONS OF OLD FRACTURES OF THE NECK OF THE FEMUR RESULTS OF TREATMENT BY VITALLIUM-MOLD ARTHROPLASTY. JBJS, 1947. 29(1): p. 41-46.
7. Judet, J. and R. Judet, The use of an artificial femoral head for arthroplasty of the hip joint. The Journal of bone and joint surgery. British volume, 1950. 32(2): p. 166-173.
8. Voorhees Jr, A.B., A. Jaretzki III, and A.H. Blakemore, The use of tubes constructed from vinyon "N" cloth in bridging arterial defects: a preliminary report. Annals of surgery, 1952. 135(3): p. 332.
9. Anderson, J.M., A. Rodriguez, and D.T. Chang. Foreign body reaction to biomaterials. in Seminars in immunology. 2008. Elsevier.

10. Sussman, E.M., et al., Porous Implants Modulate Healing and Induce Shifts in Local Macrophage Polarization in the Foreign Body Reaction. *Annals of Biomedical Engineering*, 2014. 42(7): p. 1508-1516.
11. Zhen, L. and B. Ratner, Precision-engineered Porous Material with Tunable Mechanical Property for Vascular Graft Application. 2016.
12. Wescoe, Z.L., Synthesis of Degradable poly-HEMA Hydrogels for Tissue Engineering. 2018.
13. Bandyopadhyay, A., S. Bose, and S. Das, 3D printing of biomaterials. *MRS bulletin*, 2015. 40(2): p. 108-115.
14. Chia, H.N. and B.M. Wu, Recent advances in 3D printing of biomaterials. *Journal of biological engineering*, 2015. 9(1): p. 4.
15. Jamróz, W., et al., 3D printing in pharmaceutical and medical applications—recent achievements and challenges. *Pharmaceutical research*, 2018. 35(9): p. 176.
16. Smalley, D.R. and C.W. Hull, Method of making a three dimensional object by stereolithography. 1992, Google Patents.
17. Bártolo, P.J. and I. Gibson, History of stereolithographic processes, in *Stereolithography*. 2011, Springer. p. 37-56.
18. Melchels, F.P., J. Feijen, and D.W. Grijpma, A review on stereolithography and its applications in biomedical engineering. *Biomaterials*, 2010. 31(24): p. 6121-6130.
19. Maruo, S. and K. Ikuta, Submicron stereolithography for the production of freely movable mechanisms by using single-photon polymerization. *Sensors and Actuators A: Physical*, 2002. 100(1): p. 70-76.

20. Manufacture, A., An investigation into the trueness and precision of copy denture templates produced by rapid prototyping and conventional means. *European Journal of Prosthodontics and Restorative Dentistry*, 2017. 25: p. 186-192.

21. Creff, J., et al., Fabrication of 3D scaffolds reproducing intestinal epithelium topography by high-resolution 3D stereolithography. *Biomaterials*, 2019. 221: p. 119404.

22. Serra, M., et al., A simple and low-cost chip bonding solution for high pressure, high temperature and biological applications. *Lab on a Chip*, 2017. 17(4): p. 629-634.